

# Injectable hydrogels of poly( $\epsilon$ -caprolactone-*co*-glycolide)–poly(ethylene glycol)–poly( $\epsilon$ -caprolactone-*co*-glycolide) triblock copolymer aqueous solutions

Zhiqiang Jiang<sup>a,b</sup>, Yujing You<sup>a,b</sup>, Xianmo Deng<sup>a</sup>, Jianyuan Hao<sup>a,b,\*</sup>

<sup>a</sup> Chengdu Institute of Organic Chemistry, Chinese Academy of Sciences, P.O. Box 415, Chengdu 610041, China

<sup>b</sup> Graduate School of Chinese Academy of Sciences, Beijing 100039, China

Received 5 March 2007; received in revised form 18 May 2007; accepted 1 June 2007

Available online 9 June 2007

## Abstract

Thermogelling triblock copolymers of poly( $\epsilon$ -caprolactone-*co*-glycolide)–poly(ethylene glycol)–poly( $\epsilon$ -caprolactone-*co*-glycolide) [P(CL-GA)–PEG–P(CL-GA)] were successfully prepared by control of the hydrophilicity/hydrophobicity balance and chemical compositions of the copolymers. The aqueous solutions of the copolymers underwent sol–gel transition as the temperature was increased from 20 to 60 °C. The amphiphilic copolymer formed micelles in water and a gel was formed by aggregation of micelles. The structure parameters played a critical role in determining sol–gel transition behavior. Either increasing [GA]/[CL] ratio or decreasing P(CL-GA) block length could induce the increase of the lower sol–gel transition temperature. Glycolide (GA) was incorporated into the polymer chain to increase the polymer degradation rate. Sustained release of rifampicin for approximately 32 days was obtained from the gel. It is believed to have potential applications in drug delivery and tissue engineering.

© 2007 Elsevier Ltd. All rights reserved.

**Keywords:** Hydrogels; Micelles; Phase transition

## 1. Introduction

Intelligent hydrogels which can respond to the changes in their environment, such as temperature [1,2], pH [3,4], light [5,6] and ionic strength [7,8] etc. are a class of important soft matter. Among those, biodegradable thermogelling polymers are extensively studied in the last decade for their potential applications in drug release [9,10], gene delivery [11–14], tissue engineering [15] and cell therapy etc. These thermoresponsive hydrogels used as injectable drug delivery depots have the advantages including ease of application, localized delivery for a site-specific action, prolonged delivery periods and improved patient compliance. A series of ABA or BAB

type block copolymers, in which A represents hydrophobic polyester part and B represents hydrophilic poly(ethylene glycol) part, have been reported, such as poly(ethylene glycol)/poly(lactic acid-*co*-glycolic acid) (PEG/PLGA) [16,17] and poly(ethylene glycol)/poly( $\epsilon$ -caprolactone) (PEG/PCL) [18,19]. PLGA–PEG–PLGA (commercial name: ReGel) was reported by Zentner et al. [20] as a promising commercial thermogelling copolymer. The PLGA block is biodegradable by the hydrolysis of ester bonds which can be absorbed by human body [21]. A 23% aqueous solution of this copolymer showed a sol–gel transition temperature around 20 °C and has been used to develop the sustained release formulation for anticancer drug paclitaxel.

PCL was already approved by the U.S. Food and Drug Administration (FDA) as a component of the contraceptive implant (Capronor) [22]. It is relatively hydrophobic leading to slow degradation. Polyglycolide (PGA) is also well known for non-toxicity, biocompatibility and biodegradability. It has

\* Corresponding author. Chengdu Institute of Organic Chemistry, Chinese Academy of Sciences, P.O. Box 415, Chengdu 610041, China. Tel.: +86 28 85229122; fax: +86 28 85223847.

E-mail address: [j.hao@cioc.ac.cn](mailto:j.hao@cioc.ac.cn) (J. Hao).

also been approved by FDA as a material of absorbable surgical suture, which could be completely absorbed by human body in six months. The incorporation of glycolide (GA), a fast degradation unit, into the hydrophobic PCL block can accelerate its degradation rate [23].

In this work, we report novel thermal gels composed of poly( $\epsilon$ -caprolactone-*co*-glycolide)–poly(ethylene glycol)–poly( $\epsilon$ -caprolactone-*co*-glycolide) [P(CL-GA)–PEG–P(CL-GA)] triblock copolymers with suitable sol–gel phase transition temperature. The structure–property relationship of P(CL-GA)–PEG–P(CL-GA) on the sol–gel transition was investigated.

## 2. Materials and methods

### 2.1. Materials

Poly(ethylene glycol) (PEG) with a number average molecular weight of 1540 was purchased from Chengdu Kelong Chemical Corporation and purified by recrystallization from ethyl ether. Glycolide (GA) was prepared in our lab and recrystallized from ethyl acetate before use.  $\epsilon$ -caprolactone (CL) was purchased from Acros and distilled over calcium hydride. Xylene was distilled under nitrogen after drying by refluxing over sodium. Stannous 2-ethylhexanoate was purchased from Sigma (US) without any further purification. 1,6-diphenyl-1,3,5-hexatriene (DPH) was purchased from Acros and directly used.

### 2.2. Synthesis of P(CL-GA)–PEG–P(CL-GA) triblock copolymers

The P(CL-GA)–PEG–P(CL-GA) triblock copolymers were prepared by the ring-opening polymerization of  $\epsilon$ -caprolactone and glycolide in the presence of PEG. A typical synthesis procedure is shown below. Two grams of PEG and appropriate amounts of  $\epsilon$ -caprolactone and glycolide were added into a dry flask under the protection of nitrogen. The flask was then replaced with nitrogen for at least three times to remove the moisture in monomers. Finally, the flask was added with 0.5 ml stannous octoate solution (0.01 g/ml in xylene) and 5 ml xylene, and immersed in an oil bath with predetermined temperature for 12 h. The crude product was isolated by precipitation into diethyl ether. The obtained copolymer was further purified by dissolution/precipitation from methylene chloride/ethyl ether and dried in vacuum oven at 80 °C overnight.

### 2.3. Proton nuclear magnetic resonance ( $^1\text{H}$ NMR)

An NMR spectrometer (Bruker ARX-300) was used to characterize the chemical compositions of the copolymers using  $\text{CDCl}_3$  as the solvent and investigate the micelle formation of the copolymer using  $\text{D}_2\text{O}$  as the solvent.

### 2.4. Phase transition behavior

The phase transition behavior of P(CL-GA)–PEG–P(CL-GA) aqueous solutions with different concentrations were measured by a test tube inverting method with an increment

temperature of 1 °C for each step [24]. The sample was prepared by dissolving the copolymer into distilled water in a test tube with an inner diameter of 11 mm. After incubation of the tube at 5 °C for 12 h, it was immersed in a water bath at a designated temperature for 20 min. A gel state was determined if no flow of the content was observed when inverting the tube for 1 min.

### 2.5. Micelle formation

The micellization of the copolymer in water at room temperature was studied by the dye solubilization method [25]. DPH solution (10  $\mu\text{L}$  at 0.4 mM) in methanol was injected precisely using a microsyringe into 1.0 ml P(CL-GA)–PEG–P(CL-GA) triblock copolymer solutions in a concentration range from 0.0001 to 0.316 wt%. The solutions were incubated for 6 h at room temperature (20 °C) before the measurement. The absorbance at 356 nm was plotted against polymer concentration and the crossing point of the two extrapolated straight lines was defined as CMC.

### 2.6. Dynamic mechanical analysis

The sol–gel transition of the copolymer aqueous solution was investigated using dynamic rheometry (dynamic rheometer Gemini 2000). The aqueous copolymer solution was placed between parallel plates with a diameter of 40 mm and a gap of 0.5 mm. The data were collected under a controlled stress (4.0 dyne  $\text{cm}^{-2}$ ) and a frequency of 1.0  $\text{rad s}^{-1}$  at a heating rate of 0.5 °C  $\text{min}^{-1}$ .

### 2.7. Differential scanning calorimetry (DSC)

DSC analysis was performed on a Netzsch DSC 204 F1 instrument (Netzsch GmbH) to study the thermal properties of the synthesized copolymers. The samples were first heated to 80 °C and kept at this temperature for 5 min to eliminate the thermal history. The cooling curves were recorded when the samples were cooled from 80 °C to –60 °C at a nominal rate of 10 °C/min. After keeping the samples at –60 °C for 5 min, the heating curves were recorded when they were heated from –60 °C to 80 °C at a nominal rate of 10 °C/min.

### 2.8. Wide angle X-ray diffraction (WAXD)

The wide angle X-ray diffraction (WAXD) spectra were recorded with a diffractometer (Philips X pert Pro MPD, US) with Ni-filtered  $\text{Cu K}\alpha$  radiation at room temperature. The X-ray tube worked at 40 kV and 50 mA.

### 2.9. Release of rifampicin from hydrogel in vitro

Two milligrams of rifampicin was mixed with P(CL-GA)–PEG–P(CL-GA) triblock copolymers solutions in a 10-ml test tube to form a homogeneous clear solution at room temperature. Tubes were incubated at 37 °C to form a clear gel. After 5 min, 1 ml of phosphate buffer (pH 7.4) containing  $\text{NaN}_3$

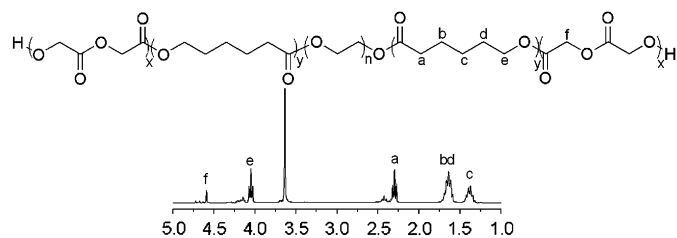


Fig. 1.  $^1\text{H}$  NMR spectrum of P(CL-GA)–PEG–P(CL-GA) triblock copolymer.

(0.02%, w/v) was added to the tubes as release medium under shaking. The amount of rifampicin in each time interval was determined by UV–vis detection at 474 nm.

### 2.10. Degradation of polymer in vitro

The aqueous solutions (25 wt%) of P(CL-GA)–PEG–P(CL-GA) were prepared in phosphate buffer saline (PBS) to form a clear aqueous dispersion. Each solution (2.0 ml) was injected into a preheated 50-ml test tube with a diameter of 2.5 cm at 37 °C.

Twenty milliliters of phosphate buffer was added to the formed gel 5 min later and shaken at 60 rpm. The samples were taken at designated time intervals, supernatant was removed, and the remaining samples were freeze-dried for 24 h. The degree of degradation was estimated from the decrease of molecular weight of the polymer.

## 3. Results and discussions

### 3.1. Synthesis and characterization of P(CL-GA)–PEG–P(CL-GA) triblock copolymers

The P(CL-GA)–PEG–P(CL-GA) triblock copolymers were synthesized by ring-opening polymerization of CL and GA monomers in xylene in the presence of PEG using stannous octoate as the catalyst. The CL and GA monomers were randomly inserted into the P(CL-GA) blocks during the polymerization process. Fig. 1 is  $^1\text{H}$  NMR spectrum of the P(CL-GA)–PEG–P(CL-GA) triblock copolymer. The peaks at 4.5–4.8 ppm, 3.6 ppm and 2.2–2.3 ppm are assigned to the GA methylene protons, the PEG methylene protons and CL  $\alpha$ -methylene protons, respectively. From these peaks, the parameters that may effect the phase transition behavior of the copolymer solutions, such as the  $[\text{EG}]/([\text{GA}] + [\text{CL}])$  ratio,  $[\text{GA}]/[\text{CL}]$  ratio, molecular weight ( $M_n$ ) and block length

of the copolymers are calculated and listed in Table 1 for ease of comparison.

### 3.2. Sol–gel transition behavior of P(CL-GA)–PEG–P(CL-GA) aqueous solutions

The effect of P(CL-GA) block length on the sol–gel transition curve for the copolymer solutions is presented in Fig. 2. PI and PIII have identical PEG block length ( $M_n = 1540$ ), similar  $[\text{GA}]/[\text{CL}]$  ratio, but different  $[\text{EG}]/([\text{GA}] + [\text{CL}])$  ratio (block length). At low temperature unimers were in equilibrium with micelles in the aqueous solution. As temperature increased the micelles bridged to form micellar groups because the hydrophobic polyester blocks can diffuse into different micelles which led to gel formation [17]. When the temperature further increased, the gel became a turbid solution due to PEG chains undergoing dehydration [26] and micellar groups precipitated in water. Longer P(CL-GA) chain in the triblock copolymers induced a stronger hydrophobic interaction, leading to an increase in the association tendency of micelles and causing bridging to occur at lower temperature. Therefore, the gel zone in the phase diagram of PI is shown to be wider than that of PIII.

The effect of  $[\text{GA}]/[\text{CL}]$  ratio on the sol–gel transition curve for the copolymer solutions is presented in Fig. 3. PI and PII have identical PEG block length ( $M_n = 1540$ ), similar  $[\text{EG}]/([\text{GA}] + [\text{CL}])$  ratio, but different  $[\text{GA}]/[\text{CL}]$  ratio. It was observed that the sol–gel temperature (LCST) increases with  $[\text{GA}]/[\text{CL}]$  ratio from 0.080 to 0.11. Since the glycolyl units are more hydrophilic than the caproyl units, the above results could be ascribed to the increased interaction of micelles with decreasing  $[\text{GA}]/[\text{CL}]$  ratio in the copolymers.

### 3.3. Micelle formation of P(CL-GA)–PEG–P(CL-GA) in aqueous solutions

The micellar state present for PI in water at room temperature was confirmed by dye solubilization experiment. The hydrophobic dye, DPH, has a very limited solubility in water and the absorbance of the solution without adding PI is very low. However, if PI is added into the water and the copolymer micelles is formed, the DPH molecules will be entrapped into the core of the micelles, which results in an increase of DPH absorbance with copolymer concentration (Fig. 4). Fig. 5 shows the critical micelle concentration (CMC) of the aqueous solution of PI at 20 °C. An abrupt increase in DPH absorbance indicates the formation of PI micelles at a critical concentration about 0.002 wt%.

Table 1  
Chemical compositions and molecular weights of the synthesized P(CL-GA)–PEG–P(CL-GA) triblock copolymers<sup>a</sup>

No.	Block length	$[\text{EG}]/([\text{GA}] + [\text{CL}])$ (mol/mol)	$[\text{GA}]/[\text{CL}]$ (mol/mol)	$M_n$ (NMR)
PI	(CL/GA) <sub>15.8/1.2</sub> –(EG) <sub>35</sub> –(CL/GA) <sub>15.8/1.2</sub>	1.03	0.080	1950–1540–1950
PII	(CL/GA) <sub>14.7/1.6</sub> –(EG) <sub>35</sub> –(CL/GA) <sub>14.7/1.6</sub>	1.07	0.111	1860–1540–1860
PIII	(CL/GA) <sub>13.5/1.1</sub> –(EG) <sub>35</sub> –(CL/GA) <sub>13.5/1.1</sub>	1.19	0.083	1670–1540–1670

<sup>a</sup> Obtained from  $^1\text{H}$  NMR analysis of the copolymers.

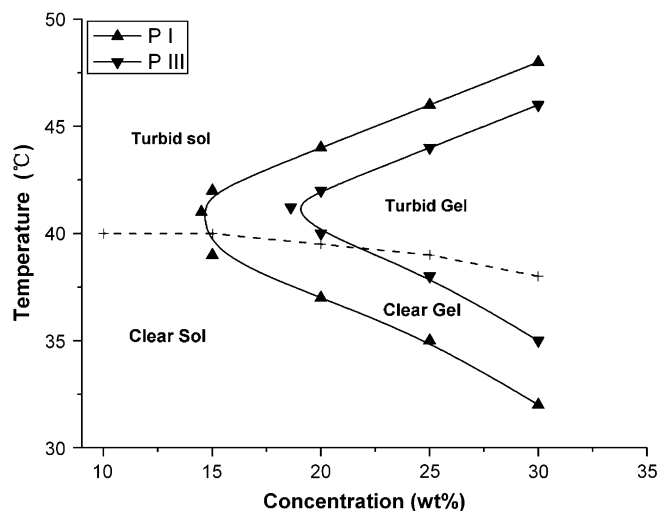


Fig. 2. Effect of P(CL-GA) block length on the sol–gel transition curve for the copolymer solutions. Increasing the P(CL-GA) block length leads to the decrease of sol–gel transition temperature.

The formation of micelles for the PI copolymer in water at room temperature was also confirmed by  $^1\text{H}$  NMR spectra in  $\text{D}_2\text{O}$  (Fig. 6). The narrow component is attributed to the more mobile shell regions, and the broad component to protons in the core regions where the mobility of chain is limited. In  $\text{D}_2\text{O}$  PEG is shown as a sharp peak while the peaks representing P(CL-GA) block is collapsed and broadened, indicating a core [P(CL-GA)]-shell (PEG) structure and slow molecular motion of P(CL-GA) segments in water. Since the critical gelation concentration (CGC) of PI (about 14%) is much higher than its CMC, micelles are formed before gelation. It suggests that the P(CL-GA)–PEG–P(CL-GA) first form micelles in the aqueous solution and then form a gel by further aggregation of micelles when a physical network is established as presented in Fig. 7.

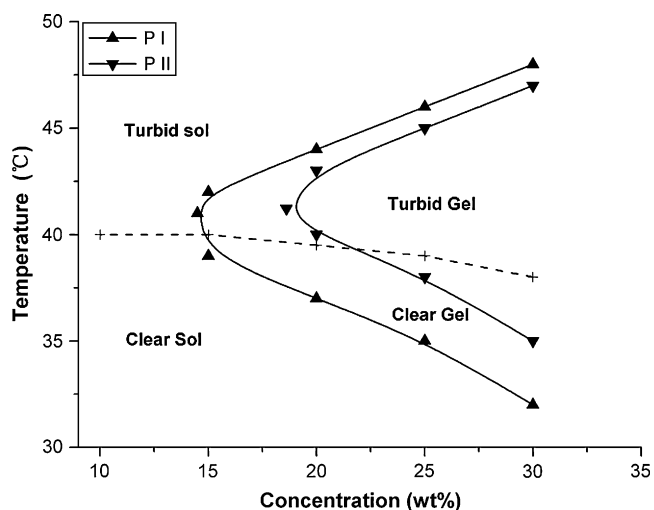


Fig. 3. Effect of [GA/CL] ratio on the sol–gel transition curve for the copolymer solutions. Increasing [GA/CL] ratio leads to the increase of sol–gel transition temperature.

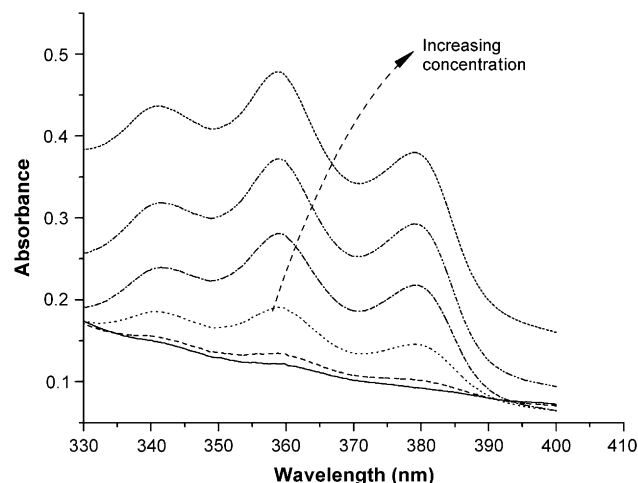


Fig. 4. UV–vis spectra of DPH as a function of PI concentration in water. Note the increase in DPH absorbance with PI concentration.

### 3.4. Dynamic mechanical analysis

The sol–gel transition for the 25 wt% aqueous solution of PI was further characterized by dynamic viscosity measurement and the result is shown in Fig. 8. The viscosity of solution at room temperature is about 0.04 Pa s, which makes it easy to formulate and inject through a syringe needle. The viscosity increases rapidly at the onset temperature of gelation ( $32^\circ\text{C}$ ) and reaches 14.9 Pa s when the gel is completely formed. Then on further increasing the temperature, the viscosity remains constant until the gel starts to collapse at  $50^\circ\text{C}$ . The change of viscosity with temperature for the 25% aqueous solution of PI shows good agreement with the sol–gel transition described previously.

### 3.5. Thermal analysis

DSC thermogram of P(CL-GA)–PEG–P(CL-GA) triblock copolymers is presented in Fig. 9. In the cooling curves of all

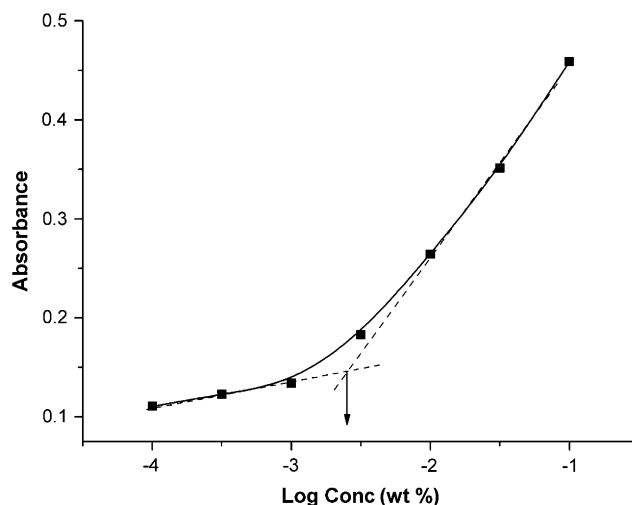


Fig. 5. Critical micelle concentration of the aqueous solution of PI measured at  $20^\circ\text{C}$ . CMC was determined by the two extrapolated lines of the absorbance at 356 nm.

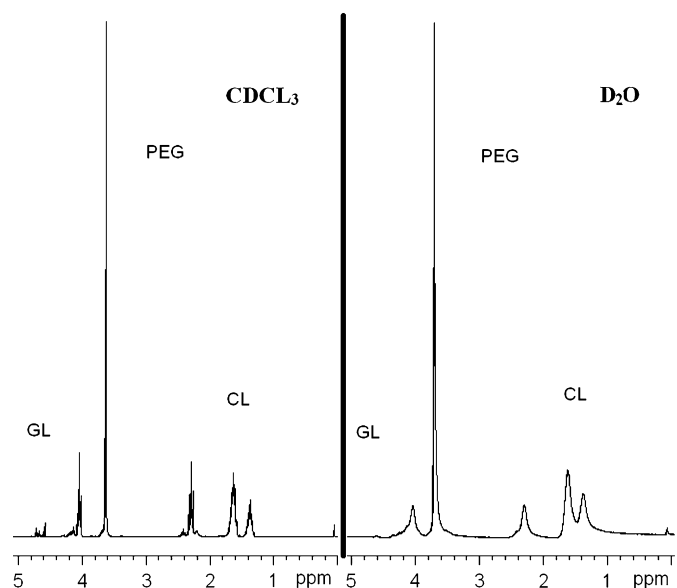


Fig. 6. Comparison of  $^1\text{H}$  NMR spectra of PI in  $\text{CDCl}_3$  and  $\text{D}_2\text{O}$  indicating a core P(CL-GA)-shell (PEG) structure.

the samples, all copolymers display a lower crystallization peak from  $-20$  to  $-10$  °C and a higher crystallization peak from  $-10$  to  $20$  °C, corresponding to the PEG and PCL component, respectively. The X-ray diffraction spectrum showed three peaks located at  $2\theta = 21.4$  and  $23.8$ , and a small shoulder at  $2\theta = 22.0$  (Fig. 10) which were assigned to crystalline regions of PCL blocks. [27] There were small diffraction peaks at  $2\theta = 19.4$  which were assigned to crystalline regions of PEG. This observation agreed with the result of thermal characterization. Despite of the similar peak temperature for PEG, the peak temperature for PCL crystallization is much higher for PI ( $14$  °C) than that for PII and PIII ( $-3$  °C). In the heating curves of Fig. 9, all copolymers have shown one melting peak at  $10$ – $20$  °C for PEG component and two melting peaks at  $25$ – $45$  °C for PCL component. The melting temperatures for the PCL component are obviously higher for PI than those for PII and PIII. It is possibly due to the existence of relatively long CL sequence in PI.

### 3.6. Release of rifampicin from hydrogel in vitro

Rifampicin was dissolved in a 25% (w/w) aqueous solution of P(CL-GA)-PEG-P(CL-GA) to form a test formulation

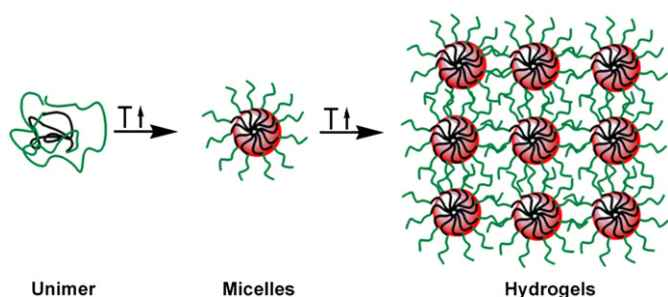


Fig. 7. Gelation mechanism of P(CL-GA)-PEG-P(CL-GA) aqueous solutions.

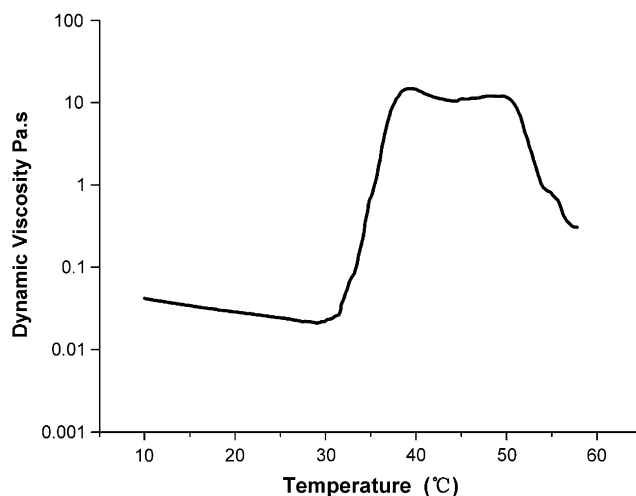


Fig. 8. Dynamic mechanical analysis of 25 wt% aqueous solution of PI as a function of temperature. Note the sharp increase in viscosity at the onset temperature of gelation ( $32$  °C).

containing 2 mg/ml rifampicin. The release profile of rifampicin from this gel is shown in Fig. 11. The release of rifampicin was consistent with a diffusion-controlled mechanism. The sustained release of the rifampicin for approximately 32 days was obtained from the gel formulation.

### 3.7. Degradation of polymer in vitro

The in vitro degradation of P(CL-GA)-PEG-P(CL-GA) was determined over a 14 week period. Upon reaching body temperature a gel was immediately formed. Between 4 and 14 weeks the physical state of the triblock copolymer changed from a gel to a mixture of a gel in a viscous liquid, and finally to a viscous liquid without gel. The molecular weight ( $M_w$ ) of retrieved polymer samples was analyzed by GPC which is

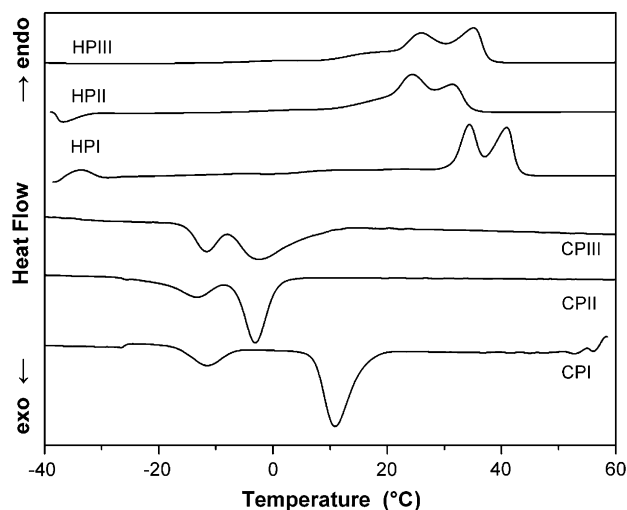


Fig. 9. DSC thermogram of P(CL-GA)-PEG-P(CL-GA) triblock copolymers. HP1, HP2, and HP3 are heating curves and CP1, CP2, and CP3 are cooling curves for the P(CL-GA)-PEG-P(CL-GA) triblock copolymer of PI, PII, and PIII, respectively.

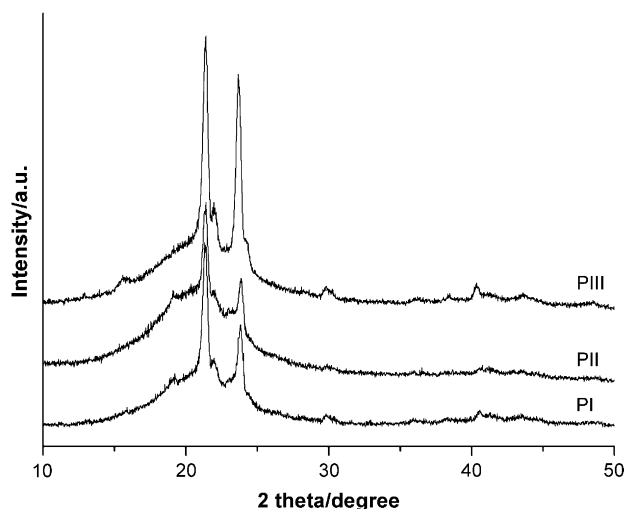


Fig. 10. XRD of P(CL-GA)-PEG-P(CL-GA) copolymers.

presented in Fig. 12. The degradation mechanism of the polyester blocks of the triblock copolymer is well known to occur by hydrolysis. The molecular weight from GPC slightly decreased upto 4 weeks of degradation indicating that chain scission by degradation did not actively occur during the first 4 weeks. After 4 weeks of degradation, 45% decrease in molar mass was observed over a 6 week period which may be ascribed to hydrolysis of fast degradable glycolide units. However, the molecular weight did not show further sharp decrease after 10 weeks due to low content of glycolide in the copolymer.

#### 4. Conclusions

Thermogelling aqueous solutions of P(CL-GA)-PEG-P(CL-GA) triblock copolymers with suitable sol-gel transition temperatures were successfully prepared. Micelles were formed in the aqueous solution of the amphiphilic copolymers and a gel was formed by aggregation of micelles. The lower

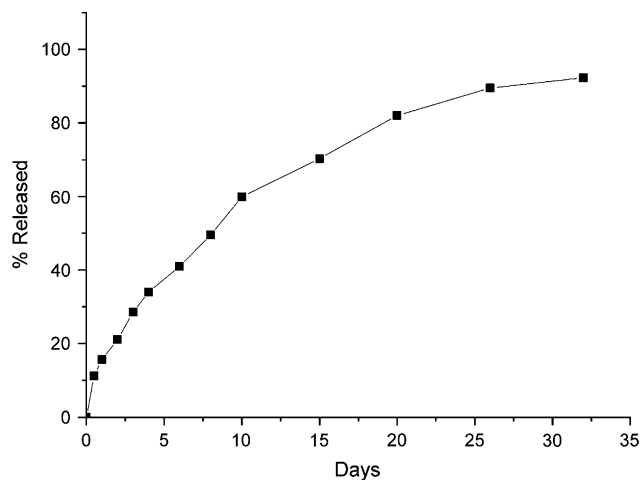


Fig. 11. Cumulative release of rifampicin from P(CL-GA)-PEG-P(CL-GA) (1950–1540–1950) triblock copolymer hydrogel.

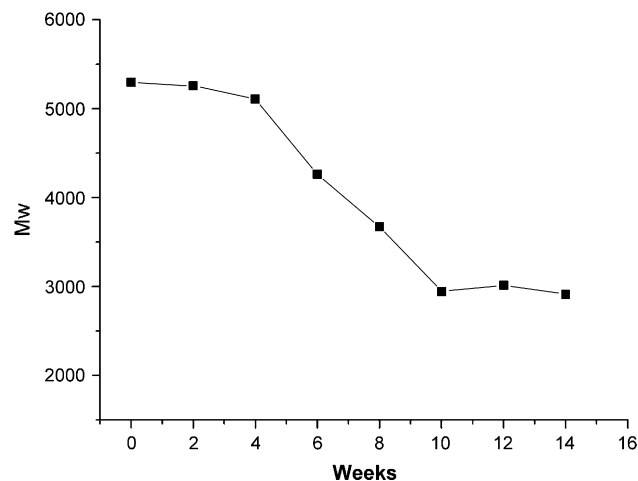


Fig. 12. The degradation behavior of P(CL-GA)-PEG-P(CL-GA) (1950–1540–1950) under pH 7.4, 37 °C.

sol-gel transition temperature can be controlled by adjusting the hydrophilicity/hydrophobicity balance of the copolymers. Increasing [GA]/[CL] ratio or decreasing the P(CL-GA) block length in the copolymers resulted in an increase of LCST. These thermal gels are useful for the formulation of injectable drug delivery depots, due to their appropriate sol-gel transition temperature and accelerated degradation.

#### Acknowledgments

This work was supported by the National Natural Sciences Fund of China (no. 50603025) and the Special Research Grant from the Dean of Chinese Academy of Sciences.

#### References

- [1] Wischerhoff E, Zacher T, Laschewsky A, Reik E. *Angew Chem Int Ed* 2000;39:4602.
- [2] Yan H, Fujiwara H, Sasaki K, Tsujii K. *Angew Chem Int Ed* 2005; 44:1951.
- [3] Moselhy J, Wu XY, Nicholov R, Kodaria K. *J Biomater Sci Polym Ed* 2000;11:123–47.
- [4] Jones CD, Lyon LA. *Macromolecules* 2000;33:8301–6.
- [5] Suzuki A, Tanaka T. *Nature* 1990;346:345–7.
- [6] Nayak S, Lyon LA. *Chem Mater* 2004;16:2623.
- [7] Duracher D, Sauzedde F, Elaissari A, Pichot C, Nabzar L. *Colloid Polym Sci* 1998;276:920–9.
- [8] Kim HJ, Lee JH, Lee M. *Angew Chem Int Ed* 2005;44:5810.
- [9] Choi S, Baudys M, Kim SW. *Pharm Res* 2004;21:827–31.
- [10] Kim YJ, Choi S, Kim SW. *Pharm Res* 2001;18:548–50.
- [11] Jeong JH, Kim SW, Park TG. *Pharm Res* 2001;21:50–4.
- [12] Li ZH, Ning W, Wang JM, Choi A, Lee PY, Tyagi P, et al. *Pharm Res* 2003;20:884–8.
- [13] Lemieux P, Guerin N, Paradis G, Proulx R, Chistyakova L, Kabanov A, et al. *Gene Ther* 2000;7:986–91.
- [14] Bochot A, Fattal E, Gulik A, Couarraze G, Couvreur P. *Pharm Res* 1998;15:1364–9.
- [15] Jeong B, Bae YH, Lee DS, Kim SW. *Nature* 1997;388:860–2.
- [16] Qiao M, Chena D, Ma X, Liu Y. *Int J Pharm* 2005;294:103–12.
- [17] Jeong B, Bae YH, Kim SW. *Macromolecules* 1999;32:7064–9.
- [18] Bae SJ, Suh JM, Sohn YS, Bae YH, Kim SW, Jeong B. *Macromolecules* 2005;38(12):5260–5.

- [19] Hwang MJ, Suh JM, Bae YH, Kim SW. *Biomacromolecules* 2005;6:885–90.
- [20] Zentner G, Rathi R, Shih C, Mcrea JC, Seo MH, Oh H, et al. *J Control Rel* 2001;72:203–15.
- [21] Wu LB, Ding JD. *Biomaterials* 2004;25:5821.
- [22] Armani ID, Liu CS. *J Micromech Microeng* 2000;10:80–4.
- [23] Li S, Dobrzynski P, Kasprczyk J. *Biomacromolecules* 2005;6:489–97.
- [24] Alexandridis P, Holzwarth JF, Hatton TA. *Macromolecules* 1994;27:2414–25.
- [25] Booth C, Attwood A. *Macromol Rapid Commun* 2000;21:501–27.
- [26] Prud'homme R, Wu KG, Dieter KS. *Langmuir* 1996;12:4651–9.
- [27] An JH, Kim HS, Chung DJ, Lee DS. *J Mater Sci* 2001;36:715–22.